Modelling atrazine sorption in carbon-rich substrates: a case study

Deborah P. Dick[a]* [ID], Larissa Z. Lara[a] [ID], Janaina B. da Costa[a] [ID], Cristiano Fontaniva[b] [ID], Ana Cristina Lüdtke[b] [ID], Heike Knicker[c] [ID]

[a] Institute of Chemistry, Federal University of Rio Grande do Sul, Porto Alegre, RS, Brazil. [b] Soil Science Department, Agronomy Faculty, Federal University of Rio Grande do Sul, Porto Alegre, Brazil. [c] Institute of Natural Resources and Agrobiology of Seville (IRNAS), Spanish National Research Council (CSIC), Seville, Spain.

Abstract: Background: The use of carbonaceous materials for environmental remediation is attractive due to low expense and high sorption capacity. However, their efficiency in contaminant removal is affected by substrate composition and sorption mechanism.

Objective: This study investigated atrazine sorption and desorption in three carbon-rich substrates. Data were evaluated considering isotherm models and sorbent chemical composition.

Methods: Sorption was performed by the batch equilibrium method with three substrates obtained from pig slurry composting with different proportions (w/w) of charcoal fines (CF): CF0, CF9 (9% CF), and CF18 (18% CF). The substrates were characterized by elemental analysis, ^{13}C NMR CP/MAS spectroscopy. The Freundlich and Dubinin-Radushkevich (DRK) models better fitted the sorption data ($0.96 > R^2 > 0.81$), followed by Temkin ($0.95 > R^2 > 0.76$). Charcoal addition to composting substrates increased carbon content and the aromaticity in the order CF0 < CF9 < CF18. However, the sorption affinity decreased in the opposite order as indicated by the Kf values: 675, 335 and 290 L kg^{-1}, respectively. Values of the E parameter (DRK) varied from 8.05 to 8.29 kJ mol^{-1}, suggesting a predominant physical sorption mechanism, whereas the Bt coefficient (Temkin) indicated an endothermic process. Desorption was only observed at higher atrazine concentrations (>10 mg L^{-1}), and the desorption Kf values were greater than the respective sorption values.

Conclusions: Atrazine sorption in the tested C-rich substrates is not governed by the carbon content or aromaticity. The low sorption reversibility implies a low atrazine mobility from the tested substrates and suggests their potential for herbicide removal in the environment.

Keywords: Composted pig slurry; Charcoal fines; Chemical composition; Isotherm models; ^{13}C NMR CP/MAS.

1. Introduction

Atrazine (2-chloro-4-ethylamino-6-isopropyl-amino-s-triazine) is one of the most common and effective soil active herbicides used to control broadleaf and grassy weeds in agriculture (Rosenfeld, Feng, 2011). In Brazil, atrazine is applied mainly on sugarcane and maize crops, two of the largest Brazilian agricultural productions, and was the fourth most used pesticide in 2020, with approximately 33.3 thousand tons of active ingredient commercialized in the country (Instituto Brasileiro de Meio Ambiente, 2021). As a consequence of this wide use, atrazine has been detected in freshwater from different regions across the country, varying greatly in concentration (from 7 to 0.004 mg L^{-1}) and often surpassing the threshold established for water potability in Brazil (2 μgL^{-1}) (Brovini et al., 2021).

One of the main processes governing pesticide dissipation after application in the field is their sorption on soil components. For mineral soils, where carbon content usually does not exceed 6% (w/w), soil organic matter (SOM) is the most relevant sorbent (Dick et al., 2010; Martins et al., 2018; Novotny et al., 2020; Piratoba et al., 2021). Therefore, sorption of pesticides is frequently related to carbon content and the addition of organic substrates as soil amendments have been used to increase the soil sorption capacity of many pesticides, thus preventing their leaching (Siedt et al., 2021). However, the chemical composition of SOM may also be influential on its interaction with pesticides. For atrazine sorption in soils, occurrence of pyrogenic carbon and the hydrophobic character of the SOM favors the herbicide retention (Dick et al., 2010; Martins et al., 2018; Alister et al., 2020; Novotny et al., 2020). Depending on the substrate type (e.g. soil, biochar, humic substances) different atrazine interaction mechanisms have been proposed, but in general, hydrogen bonding and hydrophobic partition are the most widely reported (Alister et al., 2020; Novotny et al., 2020).

The use of charred agrowaste substrates for environmental remediation has been proven to be appropriate to simultaneously give a sustainable fate to the residue as well as to provide a low-cost sorbent with a high sorption capacity (Deng et al., 2017; Mandal et al., 2017; Zhao et al., 2018). Both physical and chemical interactions for atrazine retention in biochar substrates have been

reported, and often the process is associated with the sorbent chemical and physical properties (Deng et al., 2017; Mandal et al., 2017; Zhao et al., 2018).

Besides sorption capacity, sorption mechanisms and reversibility are also important aspects to be considered when investigating pesticide behavior in the environment and the potentiality of a given sorbent to be used for environmental remediation. In the specific case of atrazine, both in soils and in carbon-rich substrates like biochar, a low desorption capacity is usually observed, thus suggesting an irreversible or strong retention by the organic sorbent (Deng et al., 2017; Martins et al., 2018; Piratoba et al., 2021).

In the present work, we investigated the potentiality of carbon-rich substrates, produced from composting of regional wastes, in removing atrazine in aqueous medium. Sorption and desorption isotherms were performed on sorbents produced from composting of pig slurry, sawdust, wood shaves and charcoal fines. The substrates were characterized by elemental analyses and ^{13}C NMR CP/MAS spectroscopy and the role of their chemical composition on the sorptive behavior was evaluated. The experimental sorption/desorption data were fitted to three sorption isotherm models (Freundlich, Temkin and Dubinin-Radushkevich). Based on the resulting parameters values, the thermodynamics and mechanism were evaluated and tentatively related to the substrate's chemical composition.

2. Material and Methods

2.1 Substrates production and their characterization

Substrates were prepared from the composting of pig slurry (PS) with sawdust (SD) and wood shavings (WS) from eucalyptus and acacia, and with charcoal fines (CF) from black acacia. The materials were obtained from a regional timber producer (SD and WS), a pig breeding farm (PS) and a charcoal plant (CF) in South Brazil. The CF used in the composting consisted of charcoal particles smaller than < 8 mm, which are not commercially viable. These particles correspond to approximately 15% of the charcoal produced in artisanal masonry ovens that provide a pyrolytic-like temperature of around 350 °C, and low oxygen concentrations.

The three composting substrates were produced in 500 L vessels into which the same amounts of PS (104 kg), WS (9kg) and SD (14kg) were added. This proportion followed the composting conditions commonly used by local farmers for fertility purposes. A mass of 11 kg or 22 kg of CF was incorporated to the reactor mass of two of the vessels to produce the CF-containing substrates (CF9 and CF18, respectively), whereas the substrate CF0 received no charcoal addition. The resulting proportions (w/w) of each material in the three substrates were:

CF0 = 82 % PS + 7 % SD + 11% WS

CF9 = 75% PS + 6% SD + 10 % WS + 9% CF

CF18 = 68 % PS + 6% SD + 8% WS + 18% CF

The samples used as sorbents were collected at 42 days of composting, air dried and macerated in an agate mortar prior to sorption experiments and analyses. For detailed information about the composting procedure and substrates analyses consult Lüdtke (2018).

The C and N contents of CF0, CF9 and CF18 were determined with an Elemental Analyzer (Perkin Elmer 2400). The pH in distilled water (pH$_{H2O}$) was measured with a pH meter (Digimed, DM-20) in the solid:solution proportion of 1:12. Specific area (SA) was determined from sorption-desorption isotherms of N$_2$ at 77 K using the Brunauer-Emmett-Teller (BET) method (Micrometrics Tristar® II 3020, USA). The solid-state ^{13}C NMR CP/MAS spectra of CF0, CF9 and CF18 were acquired with a Bruker Advance III HD 400 MHz spectrometer, operating at a resonance frequency of 100.63 MHz and using a 4 mm OD zirconium rotor with Kel-F caps. Measurements were made with a contact time of 1 ms, pulse width of ^{1}H of 90° of 2.5 μs, interval between pulses from 300 to 500 ms and accumulation of about 20,000 scans. The ^{13}C chemical shifts were calibrated relative to tetramethylsilane (0 ppm) with glycine (COOH at 176.08 ppm). The contributions of the different C groups to the total C were calculated using the MestreNova 8.1 software. The calculation was carried out considering the spinning sideband disturbance according to Knicker et al. (2005). The CPMAS ^{13}C NMR spectra were divided into four main chemical shift regions and their assignments were made accordingly Knicker et al. (2005) as follows: 0 - 45 ppm, alkyl C; 45 - 110 ppm, N/O-alkyl C + O-alkyl C; 110 - 160 ppm, aryl C; and 160-220 ppm, carboxyl/carbonyl C. Cation exchange capacity (CEC) was determined according to IN/MAPA nº 28 (Brazil, 2007) method for organic and organo-mineral fertilizers (Brasil, 2007). For comparison purposes, a pure CF sample was also characterized by the same techniques.

2.2 Sorption batch experiments

Atrazine with 98.5% purity (Syngenta Co) was used in the sorption experiments which were performed according to Dick et al. (2010). An atrazine stock solution of 100 mg L^{-1} was prepared by adding the smallest volume of HPLC-grade methanol to the pesticide mass to attain solubilization. Thereafter, the volume was completed with 0.01 mol L^{-1} CaCl$_2$ solution to simulate the soil ionic strength, which was employed in all sorption solutions. The stock solution was stored at 4 ºC in the dark.

The isotherm curve was obtained employing six initial atrazine concentrations: 0, 5, 10, 30, 50, 100 mg L^{-1}, that were prepared from the stock solution. The batch experiments were performed in duplicate at pH 7 to 7.5, using Falcon® tubes containing 0.3 g of adsorbent (CF0, CF9 or CF18) and 30 mL of atrazine solution. After 24

hours of mechanical shaking at around 25 °C (± 0.5 °C) on a light-protected horizontal orbital shaker (180 r min^{-1}), the solutions were centrifuged (1529 g for 10 min) and filtered to remove particulate matter. Atrazine in the aqueous medium was extracted with solid phase extraction (SPE), using C18 cartridges (Bound ELUT atrazine Varian and Chromabond) and then eluted with methanol HPLC-grade. The supernatant was analyzed by gas chromatography and all the experiments were carried out in duplicate. The contact time of 24 h employed presently was based on results reported in the literature about atrazine sorption and desorption on biochar or biochar amended soil, where equilibrium was reached within this timeframe (Deng et al., 2017; Mandal et al., 2017; Zhao et al., 2018).

The amount of sorbed atrazine for each isotherm point (Qe, mg g^{-1}) was calculated according to equation (1):

$$Q_e = \frac{V \times (C_0 - C_e)}{W} \tag{1}$$

Where C_0 and C_e (mg L^{-1}) represent the initial and the equilibrium atrazine concentration in the solution, respectively; V (L) is the volume of the solution; and W (g) represents the mass of the substrate.

2.3 Desorption batch experiments

After removing the sorption supernatant, the same volume (30 mL) of background solution (0.01 mol L^{-1} CaCl$_2$) was added to the falcon tube and the suspension was shaken for 24 h under the same conditions as the sorption experiment. The aqueous supernatant was removed by centrifugation and a desorption with HPLC-grade methanol was subsequently performed, following the procedure described by Kleinschmitt et al. (2006). Both aqueous and organic desorption supernatants were extracted with SPE as described earlier. The amount of desorbed atrazine was calculated by equation (2) as follows:

$$Q_{de} = \frac{(V \times C_{ed})}{W} \tag{2}$$

Where Q_{de} (mg g^{-1}) is the amount of desorbed atrazine per mass unit of sorbent; C_{ed} is the atrazine concentration desorbed in solution (mg L^{-1}). The amount of residual sorbed atrazine (Q$_R$, mg g^{-1}) was calculated as follows:

$$Q_R = Q_e - Q_{de} \tag{3}$$

2.4 Atrazine determination

The atrazine quantification in the supernatants was performed with a gas chromatograph (Shimadzu GC 2010 Plus) with a flame ionization detector (FID) equipped with Split/Splitless injector, and DB-5HT capillary column [(5% -Phenyl)-methylpolysiloxane] 30 m x 0.25 mm x 0.10 μm (Dick et al., 2010). Conditions of analyses were:

temperature of the injector at 295 °C, column at 200° C for 3.5 minutes and detector at 295 °C. The carrier gas was H$_2$ and the injection volume was 1μL of sample. The calibration curve for the atrazine quantification in the sorption/desorption experiments consisted of solutions with the same atrazine initial concentrations employed for the isotherms (from 0 to 100 mg L^{-1}). The resulting linear equation gave an R^2 of 0.9955, ensuring a linear relationship between the area of the chromatographic peak and the atrazine concentration, and excluding a possible precipitation within this concentration range.

2.5 Isotherm modeling and data treatment

The sorption equilibrium data were fitted by the following two-parameter isotherms: Freundlich, Temkin and Dubinin-Radushkevich (DRK) models. The Freundlich model assumes a multilayer sorption on a heterogeneous surface (Zhao et al., 2018) and is expressed as:

$$Q_e = K_F C_e^{\frac{1}{n}} \tag{4}$$

Or in the linearized form as

$$\ln Q_e = \ln K_F + \frac{1}{n} \ln C_e \tag{5}$$

The Freundlich constants 1/n and K$_F$ (L kg^{-1}) are used to compare the sorption intensity and sorption affinity of different sorbents (Balarak et al., 2017; Dada et al., 2012; Deng et al., 2017).

The Temkin isotherm is represented by

$$Q_e = B_t \ln (A_t C_e) \tag{6}$$

Or in the linearized form

$$Q_e = B_t \ln A_t + B_t \ln C_e \tag{7}$$

This model provides information about the sorbate-sorbent interaction and the sorption enthalpy, which is inferred from the Temkin constant B$_t$ (kJ mol^{-1}) (Dada et al., 2012). According to the model, the sorption enthalpy of all molecules in the same layer would decrease linearly rather than logarithmically with surface coverage, and an average value can be obtained from the model equation (Dada et al., 2012).

The DRK model, expressed by equation (8) or by its linearized form (9) was originally developed to account for the sorbent porosity and considers the heterogeneity of the sorption sites (Balarak et al., 2017; Hu, Zhang, 2019).

$$Q_e = Q_s \exp(-K_{ad} \varepsilon^2) \tag{8}$$

$$\ln Q_e = \ln Q_s - K_{ad} \varepsilon^2 \tag{9}$$

Where K_{ad} (mol^2 kJ^{-2}) is the DRK isotherm constant and ε is the sorption potential (10).

$$\varepsilon = RT \ln \left[1 + \frac{1}{C_e} \right] \tag{10}$$

From DRK parameters the mean free energy for the sorption process, "E" (kJ mol⁻¹), can be estimated:

$$E = \frac{1}{\sqrt{2K_{ad}}} \qquad (11)$$

Values for "E" lower than 8 kJ mol⁻¹ indicate a predominant physisorption process (as with van der Waals interactions); values between 9 and 16 kJ mol⁻¹ are indicative of chemical sorption or ion exchange (covalent or ionic bonding) whereas values between 8 and 9 kJ mol⁻¹ should represent both chemical and physisorption (Dada et al., 2012).

In order to maintain the dimensional compatibility with the calculated parameters from models, the sorption data for Temkin and DRK fitting were previously converted to mol atrazine kg⁻¹ (Qe) and mol L⁻¹ (Ce).

An approximated value for the standard Gibbs free energy (ΔG^0) (kJ mol⁻¹) of the process was estimated according equation (12) (Alister et al., 2020; Li et al., 2021):

$$\Delta G^0 = -RT \ln (K_F) \qquad (12)$$

For this calculation the Freundlich constant K_F (L kg⁻¹) was used instead of the thermodynamic equilibrium constant (which is dimensionless since it is calculated from the reagents activities) and therefore the results should not be taken as the true ΔG^0, but rather as an "approximate ΔG^0".

For comparison purposes with data reported in the literature, the distribution sorption coefficient, K_d (L kg⁻¹) was calculated from the single point approach considering the linear portion of the isotherm, according to equation (13):

$$K_d = \frac{Q_e}{C_e} \qquad (13)$$

For that, the experimental data obtained from the $C_0 = 30$ mg L⁻¹ in all substrates were employed. The index K_{oc} (L kg⁻¹), distribution coefficient normalized to the carbon content (C_T), was calculated according to equation (14).

$$K_{OC} = \frac{K_d}{C_T} \qquad (14)$$

3. Results and Discussion

3.1 Characteristics of the substrates

The C_T content of the substrate ranged from 316 g kg⁻¹ in CF0 to 378 g kg⁻¹ in CF18 (Table 1) evidencing the contribution of the charred material to the final C_T content of the substrate. The N content also increased from CF0 to CF18, however this result cannot be related to the chemical composition of added CF, since its N content is comparable to that of CF0 (Table 1). The enrichment in N verified in the CF-containing substrates is assigned to the sorption of nitrogen compounds, such as urea and uric acid, from the PS at CF surface (external

and in inner pores) during the composting process (Malińska et al., 2014). All substrates showed a basic pH level as expected due to the alkaline nature of CF (pH=9.9) and PS (pH=7.5) (Table 1). The SA and the CEC observed for CF (Table 1) were in the range of the values reported for biochar produced at low temperature and determined by the same method (Gao et al., 2019). The addition of CF to composting did not affect relevantly the SA of CF9 and CF18 but promoted a CEC decrease (Table 1). These results can be attributed to the interaction of composting material with CF, resulting in the blockage of compost surface charges without relevantly affecting their SA.

Chemical composition of CF0 determined by ¹³C CP/MAS NMR spectroscopy (Figure 1) showed the dominance of O-alkyl groups (77%) (Table 2), which indicates the presence of carbohydrate, esters, and alcohol structures. These carbon groups contribute to the hydrophilicity and ultimately to the CEC of this substrate. The addition of CF decreased the O-alkyl group proportion and increased those of aromatic C and carboxylic C (Table 2). This change in C groups distribution derives from the chemical composition of CF that is dominated by aromatic C groups and contains a relevant proportion of carboxylic C (Figure 1 and Table 2) (For detailed discussion of chemical composition of the substrates see Lüdtke, 2018).

3.2 Atrazine sorption isotherms

The atrazine isotherm plots and the corresponding linearized forms of Freundlich, Temkin and DRK models are shown in Figure 2 and the respective calculated parameters are depicted in Table 3. In general, the sorption isotherm of atrazine in the three substrates was not linear, but a saturation plateau was not achieved within the experimental conditions set (Figure 1a). The three tested models gave satisfactory fitting for the sorption data in all three substrates ($0.96 > R^2 > 0.76$) (Table 3).

3.2.1 *Freundlich Isotherm*

The calculated 1/n values ranged from 0.95 to 1.04 (Table 3), indicating that sorbate-sorbent affinity was not site-specific and did not change relevantly within the employed concentration range (Giles et al., 1960). Our results differed from those observed for atrazine sorption in pure biochar samples conducted within a smaller concentration range (0 to 10 mg L⁻¹) than the present study, where 1/n values varied between 0.41 and 0.74, indicating a strong interaction between sorbate and sorbent affinity at lower concentrations (Mandal et al., 2017). In the case of biochar amended soils, a decrease of 1/n values from 0.93 to 0.56 (Li et al., 2021) and from 0.80 to 0.54 (Deng et al., 2017) with the increase of an added amount of biochar to soil has been reported. In the cited studies, the decline in linearity (and thus an increase of sorbate-sorbent affinity) of atrazine sorption

Table 1 - pH determined in distilled water, C and N contents, C/N ratio, specific area (SA) and cation exchange capacity (CEC) of pure CF and substrates CF0, CF9 and CF18

	pH_{H2O}	C_T / (g kg⁻¹)	N / (g kg⁻¹)	C/N	SA / (m² g⁻¹)	CEC / (mmolc kg⁻¹)
CF	9.9	505.0	14.0	36.0	3.90	133.0
CF0	7.4	316.1	14.9	21.2	2.75	459.0
CF9	7.7	380.0	17.1	22.2	2.64	369.0
CF18	8.0	378.1	21.7	17.4	2.65	366.0

CF: charcoal fines; CF0: substrate without CF; CF9: substrate with 9% (w/w CF; CF18: substrate with 18% (w/w) CF
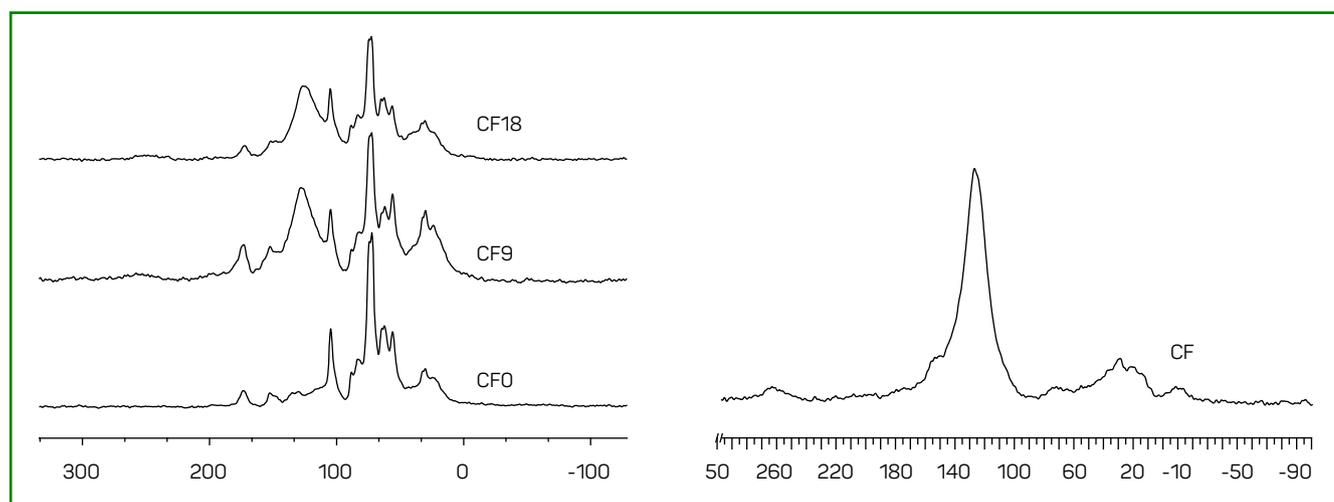
Figure 1 - Solid-state ¹³C NMR CP/MAS spectra of substrates CF0, CF9 and CF18 and of pure CF. (CF0: substrate without CF; CF9: substrate with 9% (w/w) CF; CF18: substrate with 18% (w/w) CF)

Table 2 - Distribution of carbon groups (%) determined by solid-state ¹³C NMR spectroscopy in pure CF and substrates CF0, CF9 and CF18

| Chemical shift / ppm/ proportion	Alkyl-C	N/O-Alkyl C + O-alkyl C	Aryl C	Carboxyl/ carbonyl C
	/ 0-45 (%)	/ 45-110 (%)	/ 110-160 (%)	/ 160-220 (%)
CF	14.6	6.1	68.0	6.4
CF0	15.2	76.6	7.7	0.5
CF9	19.0	42.7	31.0	7.3
CF18	14.8	50.6	32.1	2.5

CF: charcoal fines; CF0: substrate without CF; CF9: substrate with 9% (w/w CF; CF18: substrate with 18% (w/w) CF

isotherm was assigned to the increase of aromatic constituents and of heterogeneous glassy and condensed sorption domains promoted by the addition of biochar (Deng et al., 2017; Li et al., 2021). Furthermore, linear adsorption isotherms imply a partitioning mechanism whereas non-linear behavior indicates surface sorption (Li et al., 2021). Considering that in the present study, the sorption experiments were performed between pH 7 and 8, a partitioning mechanism was not unexpected since in this pH range, atrazine occurs in molecular form (Zhao et al., 2013).

The K_F values varied between 290 and 675 L kg⁻¹ and were ranked as CF0 > CF9 > CF18 (Table 3), implying a decrease in the sorption capacity with the addition of CF. The K_F values obtained in the present study were around 10² to 10³ orders of magnitude greater than those reported for soils (Alister et al., 2020; Dick et al., 2010; Martins et al., 2018; Novotny et al., 2020; Piratoba et al., 2021), and in the same order of magnitude for those reported for pyrolyzed carbon rich sorbents (Deng et al., 2017; Mandal et al., 2017; Zhao et al., 2018, 2013). Our results show that PS composted substrates (with or without addition of charred materials) may be as effective sorbents as biochar.

The "approximate ΔG^0" values were negative thus indicating that atrazine sorption in the substrates was favorable under the tested conditions. Our values are more negative than those reported for soils (Alister et al., 2020) and in the same range for values reported for biochar amended soils and hydrochar (Deng et al., 2017; Netto et al., 2022).
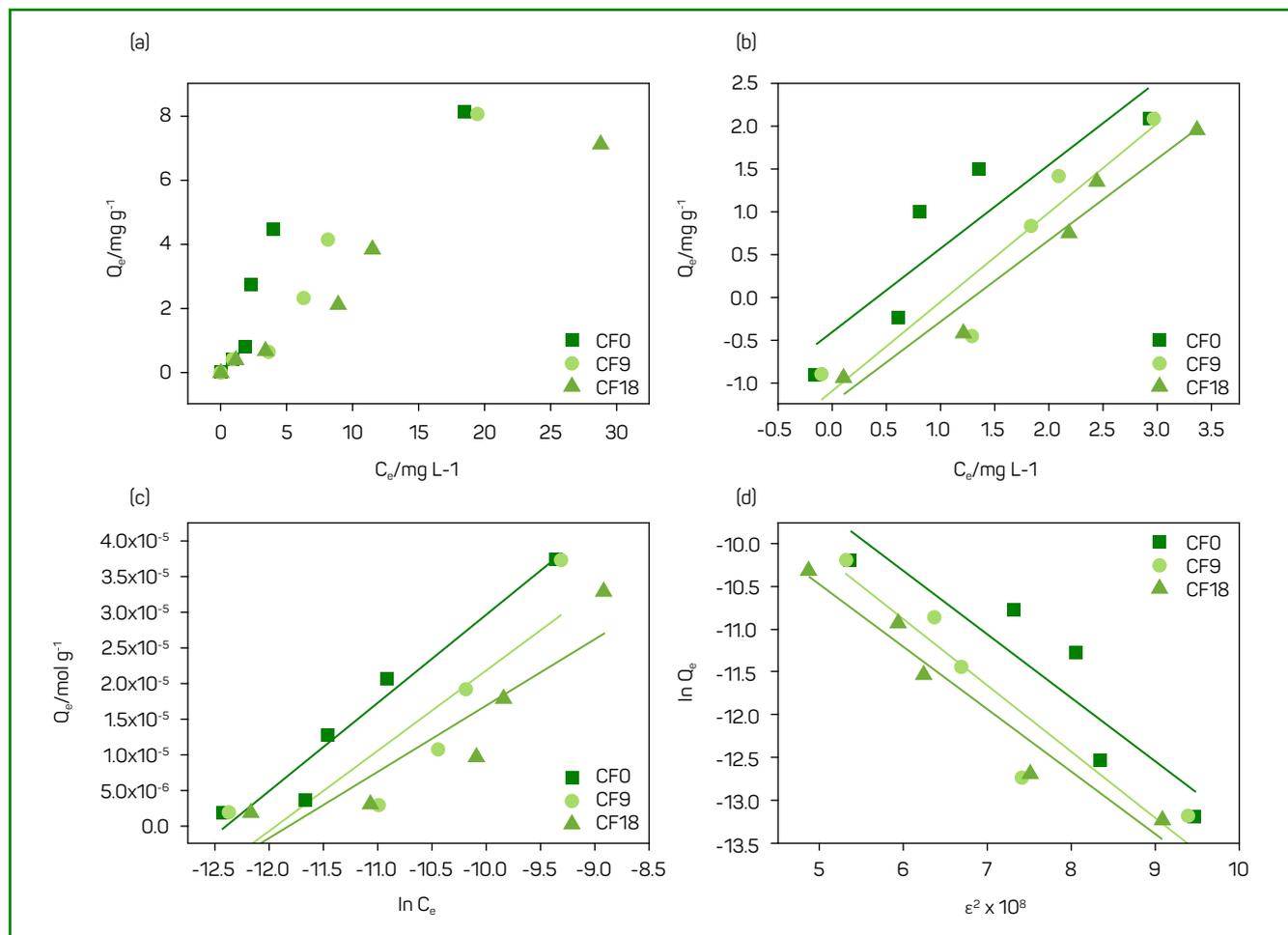
Figure 2 - Sorption isotherm of atrazine on substrates CF0, CF9 and CF18 (a) and linearized isotherm plots for Freundlich (b), Temkin (c) and Dubinin-Radushkevich (d) models. (CF0: substrate without CF; CF9: substrate with 9% (w/w) CF; CF18: substrate with 18% (w/w) CF)

3.2.2 *Temkin and DRK isotherms and thermodynamic parameters*

The positive values for Temkin B_t constant are indicative of an endothermic sorption process which agrees with the findings of Deng et al. (2017) and of Netto et al.(2022) obtained with atrazine sorption in biochar and hydrochar, respectively. The E values calculated from the DRK model ranged between 8.05 to 8.29 8 kJ mol^{-1}, thus suggesting a sorption process between atrazine and the substrates mainly through physical interactions rather than via ion exchange or chemical interactions (Balarak et al., 2017; Piccin et al., 2011).

The values of saturation capacity (Q_s) estimated from the DRK model ranged from 2.87 10^{-3} to 6.90 10^{-4} (mol g^{-1}) and correlated with the Kf values (R^2=0.77), confirming that sorption capacity decreased with the addition of CF to the substrates.

3.3 Substrates characteristics and sorption parameters

The calculated K_d decreased in the order CF0>CF9>CF18 which is in line with the pattern presented by the K_F values

(Tables 3 and 4). The inverse relationship between sorption capacity (inferred from K_F and K_d decrease) and C_T is confirmed by the obtained K_{oc} values.

In fact, K_{oc} values ranged from 622 to 3828 L kg^{-1} (Table 4) and decreased in the order CF0>CF9>CF18 indicating that CF0 displays sorption sites with greater affinity for atrazine than the other evaluated substrates. The decrease of K_d/SA in the same order, an index that informs about the density of sorption sites (Dick et al., 2010) (Table 4), confirms that assumption.

Bearing in mind that atrazine adsorbs mainly via hydrophobic interactions and hydrogen bonds (Lima et al., 2010; Martins et al., 2018; Yue et al., 2017), it would be expected that the sorption affinity would increase with the hydrophobic character of the substrates, i.e., with the increase of the proportion of aryl C + alkyl C (Table 2). However, the opposite behavior was observed. Possibly, the interaction between CF surface and composting material caused a blockage of atrazine sorptive sites in both materials, and therefore decreased the sorptive capacity of the substrate. Furthermore,

Table 3 - Isotherms parameters of Freundlich, Temkin and Dubinin-Radushkevich models determined for atrazine sorption on CF0, CF9 and CF18 substrates

Isotherm model	CF0	CF9	CF18
Freundlich			
K_F / (L kg^{-1})	674.76	334.91	290.25
1/n	0.97	1.04	0.95
R²	0.81	0.89	0.96
ΔG^0 (kJ mol^{-1})	-16.14	-14.40	-14.05
Temkin			
A_t / (L g^{-1})	1.13	0.71	0.63
B_t x 10^{-6}/ (J mol^{-1})	12.34	11.22	9.23
R²	0.95	0.76	0.82
Dubinin-Radushkevich			
Q_s / (mol g^{-1})	2.87 x10^{-3}	1.94 x 10^{-3}	6.90 x 10^{-4}
K_{ad} / (mol² J^{-2})	7.43x10^{-9}	7.72 x10^{-9}	7.82x10^{-9}
E / (kJ mol^{-1})	8.20	8.05	8.29
R²	0.84	0.87	0.95

K_F and n: Freundlich constants, B_t: Temkin constant related to sorption energy, A_t: Temkin equilibrium binding constant, Q_s: Theoretical saturation capacity, K_{ad}: Dubinin–Radushkevich constant, ε = Dubinin–Radushkevich isotherm constant; E: Mean sorption energy. CF0: substrate without CF; CF9: substrate with 9% (w/w) CF; CF18: substrate with 18% (w/w) CF

considering that CF0 presented the lowest C_T among the substrates and that SA values did not vary relevantly among the adsorbents (Table 1), these results show that for these carbon-rich composting substrates, other factors besides organic carbon content, are affecting atrazine interaction.

3.4 Desorption of atrazine

Desorption of atrazine was only detected in the aqueous extracts while the subsequent extraction with organic solvent (HPLC-grade methanol) was ineffective in extracting the pesticide under the employed conditions. The use of organic solvent after aqueous extraction had the purpose of removing atrazine from sorption sites with greater affinity than those that were desorbed with water (Leal et al., 2019). In addition, no aqueous desorption occurred for isotherm points with initial concentrations < 10 mg L^{-1} in the applied desorption conditions.

The fitting of the experimental desorption data to the Freundlich isotherm model was adequate only for the CF9 and CF18 substrates (Figure 3, Table 5). For the CF0 adsorbent, the R² coefficient for the Freundlich fitting was < 0.1 and the parameters were not calculated.

All $K_{F(d)}$ values were considerably greater than $K_{F(a)}$ (Tables 3 and 5), indicating a high retention of atrazine within 24 hours. These results suggest a low mobility of atrazine from the tested sorbents.

Table 4 - Distribution coefficients for atrazine sorption on CF0, CF9 and CF18 substrates

	K_d / (L kg^{-1})	K_{oc} / (L kg^{-1})	K_d/SA (L m^{-2})
CF0	1210	3828	0.44
CF9	368	969	0.14
CF18	235	622	0.09

Kd: distribution coefficient; Koc: distribution coefficient normalized by C_T. CF0: substrate without CF; CF9: substrate with 9% (w/w) CF; CF18: substrate with 18% (w/w) CF
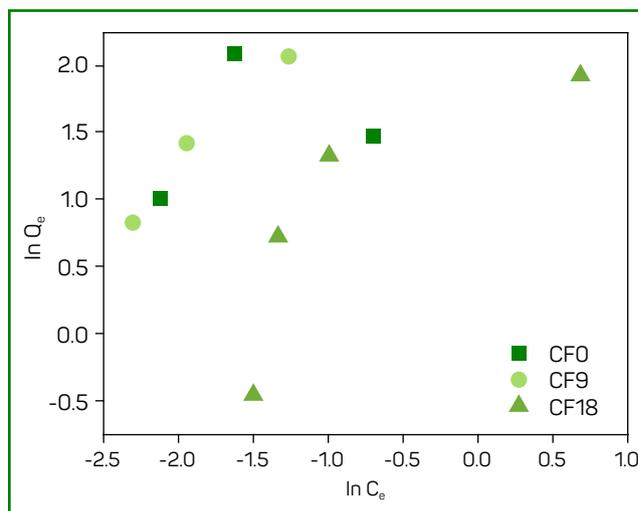
Figure 3 - Linearized Freundlich desorption isotherm plot for substrates CF0, CF9 and CF18. (CF0: substrate without CF; CF9: substrate with 9% (w/w) CF; CF18: substrate with 18% (w/w) CF)

Table 5 - Freundlich desorption parameters for CF9 and CF18

	$K_{F(d)}$ / (L kg^{-1})	1/n_d	R²
CF9	3.7 x 10^4	1,18	0,98
CF18	4.6 x 10^3	0,82	0,65

$K_{F(d)}$ and 1n/$_d$: desorption Freundlich constants. CF9: substrate with 9% (w/w) CF; CF18: substrate with 18% (w/w) CF

4. Conclusions

The C content and hydrophobicity of the sample were not the key factors in the sorption capacity and affinity of the tested substrates. For carbon-rich substrates (i.e. C content > 310 g kg^{-1}) other factors related to micromorphology take on a more important role than the chemical composition. The sorption thermodynamic parameters, calculated from the applied isotherm models, indicated that atrazine sorption in the composting substrates is an endothermic and favorable process, governed mainly by physical interactions.

The present work revealed that carbon-rich sorbents produced from PS composting with/without CF have a great potential as efficient sorbents for atrazine in environment remediation procedures. Among the tested substrates, the one without CF presented the greatest atrazine sorption capacity.

However, considering that the sorption energy (evaluated by the Bt coefficient) and the atrazine low mobility (inferred form the desorption data) were similar among the sorbents, the three tested substrates should be equally considered for waste water treatment (e.g. on-farmbio purification) or aquatic contamination. Furthermore, bearing in mind the low-cost of the precursor materials and the sustainable fate given to the wastes used in their production, this potentiality should be further investigated.

Author's contributions

All authors read and agreed to the published version of the manuscript. DPD, LZL, and JBC: conceptualization of the manuscript and development of the methodology. LZL, JBC, CF, and ACL: data collection and curation. DPD, LZL, and JBC: data analysis. DPD, LZL, and JBC: data interpretation. DPD and HK: funding acquisition and resources. DPD and HK: project administration. DPD: supervision. DPD and LZL: writing the original draft of the manuscript. DPD and LZL: writing, review and editing.

References

Alister C, Araya M, Cordova A, Saavedra J, Kogan M. Humic substances and their relation to pesticide sorption in eight volcanic soils. Planta Daninha. 2020;38:1-11. Available from: https://doi.org/10.1590/S0100-83582020380100021

Balarak D, Mostafapour F, Azarpira H, Joghataei A. Langmuir, Freundlich, Temkin and Dubinin–radushkevich isotherms studies of equilibrium sorption of ampicilin unto montmorillonite nanoparticles. J Pharm Res. 2017;20(2):1-9. Available from: https://doi.org/10.9734/jpri/2017/38056

Brazil. [Normative instruction Nr 28, from July 20, 2007. Approves the official analytical methods for analyzing substrates and soil conditioners]. Diário Oficial União. July 21, 2007. Portuguese.

Brovini EM, Deus BCT, Vilas-Boas JA, Quadra GR, Carvalho L, Mendonça RF et al. Three-bestseller pesticides in Brazil: freshwater concentrations and potential environmental risks. Sci Total Environ. 2021;771. Available from: https://doi.org/10.1016/j.scitotenv.2020.144754

Dada AO, Olalekan AP, Olatunya AM, Dada O. Langmuir, Freundlich, Temkin and Dubinin–Radushkevich Isotherms studies of equilibrium sorption of Zn 2+ unto phosphoric acid modified rice husk. IOSR J Appl Chem. 2012;3(1):38-45. Available from: https://doi.org/10.9790/5736-0313845

Deng H, Feng D, He JX, Li FZ, Yu HM, Ge JC. Influence of biochar amendments to soil on the mobility of atrazine using sorption-desorption and soil thin-layer chromatography. Ecol. Eng. 2017;99:381-390. Available from: https://doi.org/10.1016/j.ecoleng.2016.11.021

Dick DP, Martinazzo R, Knicker H, Almeida PSG. Organic matter in four Brazilian soil types: chemical composition and atrazine sorption. Quim Nova. 2010;33(1):14-9. Available from: https://doi.org/10.1590/s0100-40422010000100003

Gao Y, Jiang Z, Li J, Xie W, Jiang Q, Bi M, Zhang Y. A comparison of the characteristics and atrazine adsorption capacity of co-pyrolysed and mixed biochars generated from corn straw and sawdust. Environ. Res. 2019:172:561-8. Available from: https://doi.org/10.1016/j.envres.2019.03.010

Giles CH, MacEwan TH, Nakhwa SN, Smith D. Studies in adsorption part XI: a system. J Chem Soc. 1960;846:3973-93.

Hu Q, Zhang Z. Application of Dubinin–Radushkevich isotherm model at the solid/solution interface: a theoretical analysis. J Mol Liq. 2019;277:646-8. Available from: https://doi.org/10.1016/j.molliq.2019.01.005

Instituto Brasileiro de Meio Ambiente - IBAMA. [Pesticide marketing reports]. Brasília: Instituto Brasileiro de Meio Ambiente; 2021[access July 19th 2022]. Available From: http://www.ibama.gov.br/agrotoxicos/relatorios-de-comercializacao-de-agrotoxicos#boletinsanuais.

Kleinschmitt ARB, Dick DP, Selbach PA, Santos M. [Dessorption of the herbicide atrazine and microbial activity in two soil classes of Rio Grande do Sul State]. Cienc Rura. 2006;36(6):1794-8. Portuguese. Available from: https://doi.org/10.1590/s0103-84782006000600019

Knicker H, Totsche KU, Almendros G, González-Vila FJ. Condensation degree of burnt peat and plant residues and the reliability of solid-state VACP MAS 13C NMR spectra obtained from pyrogenic humic material. Organic Geochem. 2005:36(10);1359-77. Available from: https://doi.org/10.1016/j.orggeochem.2005.06.006

Leal DPB, Dick DP, Stahl AM, Köppchen S, Burauel P. Atrazine degradation patterns: the role of straw cover and herbicide application history. Sci Agric. 2019;76(1):63-71. Available from: https://doi.org/10.1590/1678-992x-2017-0230

Li W, Shan R, Fan Y, Sun X. Effects of tall fescue biochar on the adsorption and desorption of atrazine in different types of soil. Environ Sci Pollut Res. 2021;28:4503-14. Available from: https://doi.org/10.1007/s11356-020-10821-0

Lima DLD, Schneider RJ, Scherer HW, Duarte AC, Santos EBH, Esteves VI. Sorption desorption behavior of atrazine on soils subjected to different organic long-term amendments. J Agric Food Chem. 2010:58:3101-6. Available from: https://doi.org/10.1021/jf903937d

Lüdtke AC. [Charcoal in composting of liquid pig slurry: emission of greenhouse gases, n forms and availability in the composted for the plants] [thesis]. Porto Alegre: Universidade Federal do Rio Grande do Sul; 2018. Portuguese. Available from: https://www.ufrgs.br/agronomia/materiais/anacristinaludtke_doutorado.pdf

Malińska K, Zabochnicka-Światek M, Dach J. Effects of biochar amendment on ammonia emission during composting of sewage sludge. Ecol Eng. 2014;71:474-8. Available from: https://doi.org/10.1016/j.ecoleng.2014.07.012

Mandal A, Singh N, Purakayastha TJ. Characterization of pesticide sorption behaviour of slow pyrolysis biochars as low cost adsorbent for atrazine and imidacloprid removal. Sci Total Environ. 2017;577:376-85. Available from: https://doi.org/10.1016/j.scitotenv.2016.10.204

Martins EC, Melo VF, Bohone JB, Abate G. Sorption and desorption of atrazine on soils: the effect of different soil fractions. Geoderma. 2018;322:131–139. Available from: https://doi.org/10.1016/j.geoderma.2018.02.028

Netto MS, Georgin J, Franco DSP, Mallmann ES, Foletto EL, Godinho M et al. Effective adsorptive removal of atrazine herbicide in river waters by a novel hydrochar derived from Prunus serrulata bark. Environ Sci Pollut Res. 2022;29:3672-85. Available from: https://doi.org/10.1007/s11356-021-15366-4

Novotny EH, Turetta APD, Resende MF, Rebello CM. The quality of soil organic matter, accessed by 13C solid state nuclear magnetic resonance, is just as important as its content concerning pesticide sorption. Environ Pollut. 2020;266(part 1):115298. Available from: https://doi.org/10.1016/j.envpol.2020.115298

Piccin JS, Dotto GL, Pinto LAA. Adsorption isotherms and thermochemical data of FDandC RED N° 40 Binding by chitosan. Brazilian J Chem Eng. 2011;28(2):295-304. Available from: https://doi.org/10.1590/S0104-66322011000200014

Piratoba ARA, Miranda Junior MS, Marulanda NME, Pereira GAM, Lima CF, Silva AA. Sorption and desorption of atrazine in horizons of the red-yellow latosol. Adv Weed Sci. 2021:39:021219156. Available from: https://doi.org/10.51694/AdvWeedSci/2021;39:00003

Rosenfeld PE, Feng LGH. Pesticides. In: Rosenfeld P, Feng L. Risks of hazardous wastes. Amsterdam: Elsevier; 2011. p. 127-54.

Siedt M, Schäffer A, Smith KEC, Nabel M, Roß-Nickoll M, van Dongen JT. Comparing straw, compost, and biochar regarding their suitability as agricultural soil amendments to affect soil structure, nutrient leaching, microbial communities, and the fate of pesticides. Sci Total Environ. 2021;751:141607. Available from: https://doi.org/10.1016/j.scitotenv.2020.141607

Yue L, Ge CJ, Feng D, Yu H, Deng H, Fu B. Adsorption–desorption behavior of atrazine on agricultural soils in China. J Environ Sci. 2017;57:180-9. Available from: https://doi.org/10.1016/j.jes.2016.11.002

Zhao L, Yang F, Jiang Q, Zhu M, Jiang Z, Tang Y et al. Characterization of modified biochars prepared at low pyrolysis temperature as an efficient adsorbent for atrazine removal. Environ Sci Pollut Res. 2018;25:1405-17. Available from: https://doi.org/10.1007/s11356-017-0492-2

Zhao X, Ouyang W, Hao F, Lin C, Wang F, Han S et al. Properties comparison of biochars from corn straw with different pretreatment and sorption behaviour of atrazine. Bioresour Technol. 2013:147:338-44. Available from: https://doi.org/10.1016/j.biortech.2013.08.042